Alkalinity of the Mediterranean Sea

Anke Schneider,[1] Douglas W. R. Wallace,[1] and Arne Körtzinger[1]

Received 27 November 2006; revised 16 May 2007; accepted 7 June 2007; published 11 August 2007.

[1] Total alkalinity (A_T) was measured during the Meteor 51/2 cruise, crossing the Mediterranean Sea from west to east. A_T concentrations were high ($\sim$2600 μmol kg^{-1}) and alkalinity-salinity-correlations had negative intercepts. These results are explained by evaporation coupled with high freshwater A_T inputs into coastal areas. Salinity adjustment of A_T revealed excess alkalinity throughout the water column compared to mid-basin surface waters. Since Mediterranean waters are supersaturated with respect to calcite and aragonite, the excess alkalinity likely reflects alkalinity inputs to coastal areas close to regions of deep and intermediate water formation. An alkalinity budget shows that main alkalinity inputs come from the Black Sea and from rivers, whereas the Strait of Gibraltar is a net sink. The major sink appears to be carbonate sedimentation. The basin-average net calcification rate and $CaCO_3$ sedimentation was estimated to be 0.38 mol m^{-2} yr^{-1}. The estimated residence time of A_T is $\sim$160 yr.
Citation: Schneider, A., D. W. R. Wallace, and A. Körtzinger (2007), Alkalinity of the Mediterranean Sea, *Geophys. Res. Lett.*, *34*, L15608, doi:10.1029/2006GL028842.

1. Introduction

[2] The Mediterranean Sea is a semi-enclosed basin, connected to the Atlantic Ocean via the Strait of Gibraltar. The inflowing low-nutrient Atlantic water is responsible for its generally oligotrophic and relatively well oxygenated character. Due to insolation and resulting evaporation on the one hand and little precipitation and river discharge on the other, the Mediterranean Sea has a negative freshwater balance resulting in an anti-estuarine thermohaline circulation. The classical circulation is schematically described as an open thermohaline cell with two deep-reaching closed secondary cells [*Lascaratos et al.*, 1999]. The principal cell pictures the transformation of inflowing Atlantic Water (AW) at the surface to outflowing Levantine Intermediate Water (LIW): on its way eastwards, the AW becomes warmer and saltier, forming Modified Atlantic Water (MAW). In winter chilly winds cool the surface waters in the Levantine basin making them dense enough to sink and mix with underlying water [*Ovchinnikov*, 1984]. At intermediate depths the now called LIW flows back to the west. The two secondary cells describe the development of Eastern and Western Mediterranean Deep Waters, once again driven by strong evaporation and cooling of surface waters in the Adriatic and the Gulf of Lyon, respectively [*Gascard*, 1978; *Pollak*, 1951]. In 1988, with the development of a new deep water component originating in the Aegean Sea, the 'classical circulation' changed from a single deep water source in the Eastern Mediterranean to a two source system [*Roether et al.*, 1996]. Since then a major portion of the former bottom water in the Eastern Mediterranean has been uplifted and replaced by this very dense Aegean water [*Klein et al.*, 1999].

[3] Due to the sparseness of measurements, especially in the eastern basin, little is known about the carbonate system of the Mediterranean Sea. Published data for total alkalinity (A_T) are spatially and temporally limited [*Copin-Montégut*, 1993; *Copin-Montégut and Bégovic*, 2002; *Millero et al.*, 1979] and make it difficult to draw a coherent picture of the alkalinity distribution. Here we present a new, broad and reliable dataset for A_T which covers primarily the eastern basin (Figure 1) and allows a reasonable estimate of the alkalinity budget.

2. Materials and Methods

[4] Measurements of salinity, temperature and oxygen were made at 42 stations along the cruise track of R/V Meteor cruise 51/2 (M51/2, 18 October – 11 November 2001, Malaga – La Valetta), crossing the Mediterranean Sea from west to east. Measurements of A_T and total dissolved inorganic carbon (DIC) were made at 14 stations using potentiometric titration [*Mintrop et al.*, 2000] and coulometric titration [*Johnson et al.*, 1993] methods, respectively. Water samples were taken from Niskin bottles in 500 mL Duran glass bottles and poisoned with 100 μL of saturated aqueous solution of mercuric chloride for later shore-based analysis. The results of the DIC measurements will be presented elsewhere. (Data are available from the database CDIAC, http://cdiac.ornl.gov).

[5] The accuracy of the A_T determination was assessed by regular measurements of Certified Reference Material (CRM, supplied by Andrew Dickson, Scripps Institution of Oceanography (SIO), La Jolla, CA, USA). The A_T concentration of each CRM batch is certified by shore-based potentiometric titration [*Dickson*, 1998; *Dickson et al.*, 2003]. A_T measurements on CRMs from 2 batches (batch # 48 and 52) yielded a mean offset between our measurements and the certified values of -0.82 ± 2.85 μmol kg^{-1} (95% confidence interval, n = 41). Measured A_T concentrations were therefore adjusted to the certified values by correction for this mean offset. Precision of the A_T measurements was 4.2 μmol kg^{-1} (95% confidence interval), determined from duplicate samples (n = 15).

[6] The degree of saturation (Ω) for calcite and for aragonite was calculated from A_T and DIC with the software program CO2SYS [*Lewis and Wallace*, 1995], using the carbonic acid dissociation constants (K_1 and K_2) from *Mehrbach et al.* [1973] as refitted by *Dickson and Millero*

[1]Forschungsbereich Marine Biogeochemie, Leibniz-Institut für Meereswissenschaften, IFM-GEOMAR, Kiel, Germany.

0094-8276/07/2006GL028842$05.00

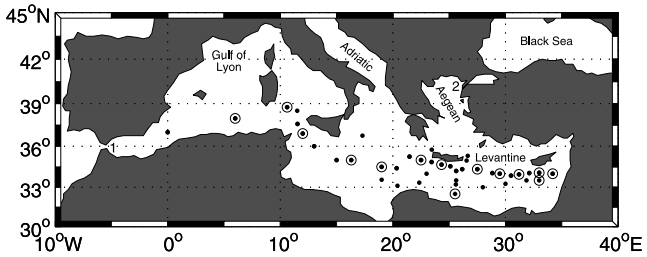

Figure 1. Station plot of the Meteor 51/2 cruise in October/November 2001. Encircled dots indicate stations where alkalinity and DIC measurements were made. 1: Strait of Gibraltar; 2: Dardanelles.

[1987] and the dissociation constant for HSO_4^- from *Dickson* [1990].

3. Results and Discussion

3.1. Alkalinity Distribution

[7] Figure 2a shows the relatively homogeneous distribution of A_T throughout the water column (salinity-adjusted alkalinities shown in Figure 2b are described later). Concentrations are high, reflecting the high salinity of the Mediterranean Sea and are typically $\sim$2600 μmol kg^{-1}. Two exceptions are 1) the MAW with lower salinities and accordingly lower A_T, and 2) the western basin with alkalinities around 2580 μmol kg^{-1}, which also can be attributed to slightly lower salinity.

[8] Figure 3a displays the linear relationships between A_T and salinity (S). In surface waters (depth < 25 m) A_T shows the following correlation with S:

$$A_T = 73.7(\pm 3.0) \cdot S - 285.7(\pm 114.94)\ \mu\text{mol kg}^{-1} \quad (n = 15, r^2 = 0.98, \sigma_y = 8.20). \tag{1}$$

[9] Although previous authors have reported negative intercepts of the A_T-S relationship in the Mediterranean A_T-S regression, no explanation has been given for this unusual feature. The negative intercept can be explained by exceptional circumstances in the Mediterranean, namely: high evaporation and high alkalinity of freshwaters entering the basin by rivers and the Black Sea. These processes are represented by vectors in Figure 3b. Starting point for our considerations is the inflow of Atlantic water from the west (A), which is low in both A_T and S. Disregarding other effects, evaporation would drive a steady increase in S and A_T during the surface waters' movement towards the east. The corresponding theoretical evaporation line (evap) on the A_T-S diagram would run through the origin (S = 0; A_T = 0). The second major influence on Mediterranean water alkalinity is A_T addition by rivers and by the Black Sea: both carry very high alkalinities (between 2000 μmol kg^{-1} and 6500 μmol kg^{-1}) at low or zero salinity. These inputs occur in coastal areas and in the eastern basin, respectively, where surface S and A_T tend to be highest due to the cumulative effects of evaporation. Hence on the A_T-S diagram the influence of coastal alkalinity inputs occurs towards the high-salinity-end of the evaporation line, e.g. at the hypothetical point B with a maximum salinity of 40 on Figure 3b. Accordingly, mixing between high salinity surface water (B) and river or Black Sea water, with their respective endmembers, shifts the characteristics of surface waters towards lower S and higher A_T, i.e. in the direction of the arrows for "riv" and "bs". As a result, the mixture of Mediterranean surface water does not follow a pure evaporative line on an A_T-S diagram but reflects this admixture of high-A_T, low-S endmembers. Consequently, in Figure 3b the mixing lines "riv", "bs" and "evap" picture the boundaries between which our data points should fall and one can observe that most measured samples do lie between these boundaries. Towards lower salinities (i.e. in the western basin) the surface A_T-S relationship of our samples matches the evaporation line rather well, and no clear influence of the high A_T endmembers can be observed. In contrast, at salinities greater than 38, i.e. in the eastern basin and in marginal seas, this effect starts to appear and the deviations from the evaporation line increase with increasing salinity.

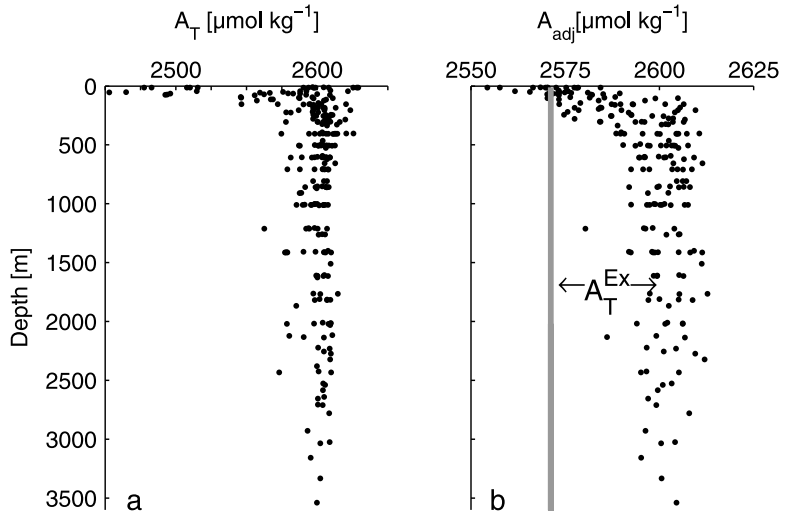

Figure 2. Scatter plot of (a) total alkalinity and (b) salinity adjusted alkalinity for all water samples taken during M51/2. A_T^{Ex} represents the excess alkalinity in deep water as compared to the average surface alkalinity.

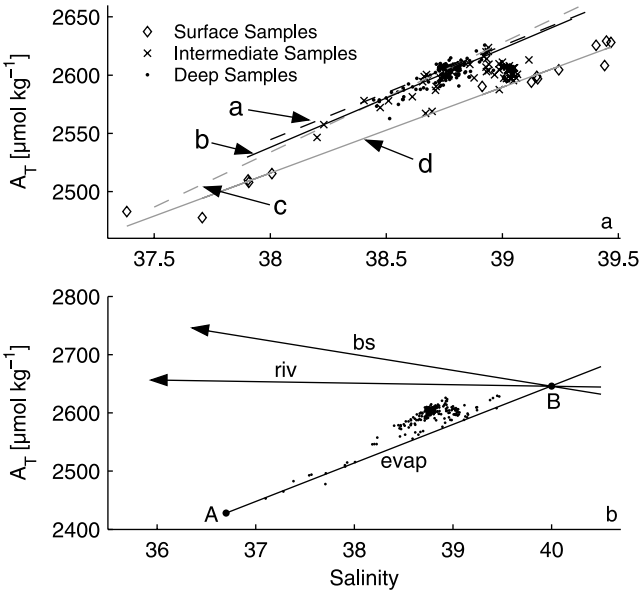

Figure 3. (a) A_T-S-correlation of samples from all stations. Surface samples reach from 0-25 m, intermediate depth samples from 100-400 m and deep samples are below 400 m. The grey line (d) shows the surface regression and the black line (b) the deep regression of the samples. The dashed lines (a and c) show the correlations between alkalinity and salinity at the Dyfamed Site (grey (c) = surface regression, black (a) = deep regression) reported by *Copin-Montégut and Bégovic* [2002]. Linear equations are displayed in the text. (b) Demonstration of evaporation and mixing processes in the Mediterranean Sea as described in the text. Atlantic water (A) evaporates (evap) and high salinity water (B) mixes with riverine (riv) and Black Sea (bs) water. All samples from M51/2 plot well within the A_T-S diagram (black datapoints).

Hence the observed A_T-S relationship in the Mediterranean is steeper than the evaporation line and yields a negative intercept. It is worthwhile to reiterate that this intercept is not representative of any endmember component but a consequence of the presence of high-A_T, low-S influence in the central basin.

[10] The correlation found for deep waters (depth > 400 m) is:

$$A_T = 84.7(\pm 4.89) \cdot S - 682.1(\pm 189.37)\ \mu\text{mol kg}^{-1} \quad (2)$$
$$\left(n = 152, r^2 = 0.67, \sigma_y = 5.54\right),$$

which suggests an enhanced influence of high alkalinity coastal waters in the deep basins. Within the error bars the deep water relationship (Equation (2)) is in agreement with the relationship observed by *Copin-Montégut and Bégovic* [2002] at the Dyfamed Site in the NW Mediterranean Sea below 500 m ($A_T = 80.62 \cdot S - 518.96\ \mu\text{mol kg}^{-1}$). In contrast, the surface water regression line of *Copin-Montégut and Bégovic* [2002] ($A_T = 93.996 \cdot S - 1038.1\ \mu\text{mol kg}^{-1}$) differs from ours (Equation (1)). The reason for the less steep slope and the less negative intercept of our correlation (Equation (1)) likely reflects the different sampling locations. The Dyfamed Site is located in the north-western Mediterranean Sea (43°25′N, 07°52′E) and likely more coastally-influenced than most of our stations. In coastal regions, alkalinity inputs from rivers (e.g. the nearby Rhone River with a mean alkalinity of 2885 μmol kg^{-1}, Table 1) and potentially from the sediments cause the steeper slope of the regression line.

[11] In order to compensate for salinity-driven variations, A_T was adjusted to a reference salinity ($S_{ref} = 38.75$) which is the mean surface salinity of our samples. The adjusted alkalinity (A_{adj}, Figure 2b) was calculated according to *Friis et al.* [2003]: $A_{adj} = [(A_T - A_T^{S=0})/S] \cdot S_{ref} + A_T^{S=0}$. This equation includes the non-zero intercept ($A_T^{S=0} = -286\ \mu\text{mol kg}^{-1}$) resulting from our surface A_T-S relationship (Equation (1)). Excess alkalinity (A_T^{Ex}) is defined as the difference between a given sample's alkalinity (adjusted to $S_{ref} = 38.75$) and the surface ocean reference alkalinity of 2571.2 μmol kg^{-1} (mean alkalinity in the upper 25 m at the mean salinity of 38.75). Overall we find positive values for A_T^{Ex} throughout the sub-surface, which means that, independent of salinity variations, the entire water column is enriched in alkalinity relative to the upper 25 m. The highest excess values were found in the eastern basin. At around 27°E, surface properties extend down to about 300 m depth, which could be the result of the anticyclonic Iera Petra Gyre in this region. This feature was also observed in other parameters (e.g. temperature and oxygen).

[12] A surface-to-depth increase of A_T^{Ex} would be expected, if calcifying organisms removed alkalinity from the photic zone and dissolution of calcium carbonate added alkalinity at depth. However, within the Mediterranean A_T^{Ex} remains constant below ~300 m at about 30 μmol kg^{-1} (Figure 2b). Furthermore, calculation of calcite and aragonite saturation states reveals that Mediterranean waters are strongly supersaturated ($\Omega > 1$) with respect to both minerals throughout the entire water column (Figure 4). Hence dissolution of calcium carbonates is not favoured thermodynamically. The degree of saturation for calcite lies

Table 1. Discharge and Mean A_T of Six Main Rivers Discharging Into the Mediterranean[a]

River	Discharge km^3 yr^{-1}	Reference	Mean A_T μmol L^{-1}	Reference
Rhone	49.5	GEMSWATER, 2002[b]	2885	GEMSWATER, 2002[b]
Po	46.7	GEMSWATER, 2002[b]	2918	GEMSWATER, 2002[b]
Nile	30.0	GEMSWATER, 2002[b]	2213	GEMSWATER, 2002[b]
Ebro	17.4	GEMSWATER, 2002[b]	2148	GEMSWATER, 2002[b]
Tiber	7.2	Vorosmarty et al., 1998[c]	6600	*Copin-Montégut* [1993]
Adige	7.2	Vorosmarty et al., 1998[c]	2100	*Copin-Montégut* [1993]

[a]Total discharge of these six rivers is 158 km^3 yr^{-1} (nearly one third of the overall river discharge into the Mediterranean Sea) and the mean discharge-weighted A_T is 2820 μmol L^{-1}.
[b]GEMSWATER 2002: Water quality data tables for 82 major river basins, 2006, from www.gemswater.org/atlas-gwq/intro.e.html.
[c]Vorosmarty et al., 1998: Global River Discharge Database (RivDIS) V. 1.1, 2006, from http://www-eosdis.ornl.gov.

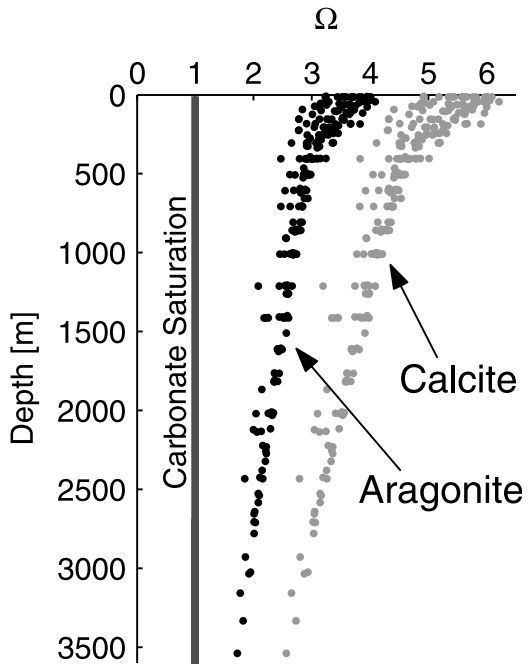

Figure 4. Vertical profiles of the saturation state (Ω) of calcite and aragonite in the Mediterranean Sea.

between 5 and 6 at the surface and ~2.5 at 3500 m depth. For aragonite it ranges between 3 and 4 at the surface and ~1.5 at depth. Similar observations have been reported previously for the western, the central and the eastern basins [*Millero et al.*, 1979, and references therein].

[13] We hypothesise that the inflow of high alkalinity water from rivers as well as from the Black Sea contributes to both the observed A_T^{Ex} and the high saturation state of deep waters, with the high alkalinity arising from weathering of limestone in adjacent areas. Deep water formation in marginal seas appear to rapidly transport coastal alkalinity anomalies directly into the deep basins where they show up as A_T^{Ex}, thereby effectively bypassing the surface waters of the central Mediterranean (to which A_T^{Ex} is referenced). As our stations were located mainly in the mid-basin, our surface water samples were heavily influenced by the inflowing AW with lower alkalinity. A_T measurements from coastal and marginal seas, and especially in the areas of deep water formation, are needed to test this hypothesis. In the absence of such data, it cannot be ruled out that dissolution of readily soluble high magnesium carbonates and other carbonate particles within the water column above the saturation horizon might also contribute to deep water excess alkalinity. Anyway, little is known about these processes and because of the high saturation state throughout the water column in the Mediterranean Sea, carbonate dissolution seems unlikely and is not further considered here.

3.2. Alkalinity Budget

[14] We compiled an alkalinity budget in order to quantify sources and sinks as well as the turnover time of A_T in the Mediterranean Sea. The Mediterranean Sea alkalinity is controlled by water exchange with the Atlantic and the Black Sea, as well as by riverine inputs, and sedimentation of calcium carbonate. With the exception of the sedimentary sink, all net fluxes can be calculated from published estimates of the volumes of inflowing and outflowing water and measurements or estimates of their corresponding alkalinity concentrations (Table 2). Local alkalinity values were estimated from salinity data and an appropriate regional A_T-S regression correlation. The alkalinity of water leaving the Mediterranean towards the Black Sea was estimated from the A_T-S correlation of the surface waters presented in this paper (Equation (1)). A_T entering the Mediterranean through the Dardanelles from the Marmara Sea was estimated from A_T concentrations of water leaving the Black Sea [*Hiscock and Millero*, 2006, Figure 6] and consideration of the subsequent salt and alkalinity divergence within the Marmara Sea [*Besiktepe et al.*, 1994]. The alkalinity of water leaving the Mediterranean Sea through the Strait of Gibraltar was estimated using an A_T-S correlation obtained from our measurements in the western LIW. The mean alkalinity of the inflowing Atlantic water was determined via a relationship published by *Lee et al.* [2006] of A_T with salinity and temperature for the North Atlantic. Finally a mean river alkalinity was estimated from the discharge-weighted alkalinities of six main rivers discharging into the Mediterranean (Table 1). The estimated values of the mean alkalinities in Table 2 have uncertainties and our estimates require verification through direct measurements.

[15] All fluxes at the interfaces of the Mediterranean Sea are listed in Table 2. Main contributors of A_T are the Black Sea and rivers, whereas the Strait of Gibraltar is a net sink for alkalinity. Compared to the findings of *Copin-Montégut* [1993] who estimated a net alkalinity flux of $2.43 \cdot 10^{12}$ mol yr^{-1} into the Atlantic, we obtained a much lower export ($0.8 \cdot 10^{12}$ mol yr^{-1}), which accounts for only about one third of the net A_T inputs. If we assume Mediterranean Sea alkalinity to be in steady state, long term net inputs of alkalinity must equal long term sinks, for which

Table 2. Water, Salinity, and Alkalinity Exchange of the Mediterranean Sea With the Atlantic, the Black Sea, and Rivers[a]

	In/Out	Water Volume, $km^3\ yr^{-1}$	Mean Salinity	Mean A_T, $\mu mol\ L^{-1}$	Salt-Flux, $kg\ yr^{-1} \cdot 10^{13}$	A_T Flux, $mol\ yr^{-1} \cdot 10^{12}$	
Atlantic Ocean	in	22706[b]	36.1[b]	2436	+82.0	+55.3	net flux −0.8
	out	21444[b]	38.2[b]	2617	−81.9	−56.1	
Black Sea	in	1218[c]	29.3[c]	2967	+3.6	+3.6	net flux +1.2
	out	918[c]	38.9[c]	2643	−3.6	−2.4	
Rivers	in	513[d]	0	2820	0	+1.5	net flux +1.5

[a]Here "in" refers to water flowing into the Mediterranean and "out" to water escaping the basin. Mean A_T values were estimated as described in the text.
[b]*Bryden et al.* [1994].
[c]*Besiktepe et al.* [1994].
[d]*Tixeront* [1969].

only sedimentation appears to be a reasonable candidate. Under this assumption, the alkalinity loss via carbonate sedimentation amounts to $\sim 1.9 \cdot 10^{12}$ mol yr^{-1}. When distributed equally across the Mediterranean basin (surface area of $2.5 \cdot 10^{12}$ m^2 [*Menard and Smith*, 1966]) this alkalinity loss corresponds to a surface ocean calcification rate of 0.38 mol m^{-2} yr^{-1} (neglecting water column carbonate dissolution). Recently published data for the carbonate flux in the NW Mediterranean [*Martin et al.*, 2006] are consistent with this estimate: For example, whereas sediment traps in the Palamós submarine canyon showed very high carbonate fluxes close to the coast (up to 40 mol m^{-2} yr^{-1}), the values decreased with increasing distance from the coast. The farthest-offshore mooring (depth = 1300 m) showed a mean annual flux of 0.40 mol m^{-2} yr^{-1}, which corresponds to our estimate.

[16] An A_T inventory of the Mediterranean Sea was estimated by integrating the mean depth profile of alkalinity over the average basin depth of 1500 m [*Menard and Smith*, 1966] and by scaling the resulting column inventory to the surface area of the entire basin. With a calculated A_T inventory of $9.7 \cdot 10^{15}$ mol, the residence time (τ) of alkalinity in the basin is $\sim$160 yr. For comparison, we determined a salt inventory ($2.42 \cdot 10^{17}$ kg) and a residence time for salt ($\tau \cong 280$ yr) in the same manner as for alkalinity. As expected, the residence time for salinity is longer than that of A_T.

[17] **Acknowledgments.** We thank the crew of R/V Meteor for their assistance, Peter Streu and Tobias Steinhoff for collection and measurement of the samples. Thanks also to Birgit Klein for helpful discussions and to Wolfgang Roether, the Chief Scientist of the cruise. Funding for this work was provided by the CarboOcean IP of the European Commission (grant 511176-2) and by the Deutsche Forschungsgemeinschaft (DFG).

References

Besiktepe, S. T., H. I. Sur, E. Ozsoy, M. A. Latif, T. Oguz, and U. Unluata (1994), The circulation and hydrography of the Marmara Sea, *Prog. Oceanogr.*, *34*(4), 285–334.

Bryden, H. L., J. Candela, and T. H. Kinder (1994), Exchange through the Strait of Gibraltar, *Prog. Oceanogr.*, *33*(3), 201–248.

Copin-Montégut, C. (1993), Alkalinity and carbon budgets in the Mediterranean Sea, *Global. Biogeochem. Cycles*, *7*(4), 915–925.

Copin-Montégut, C., and M. Bégovic (2002), Distributions of carbonate properties and oxygen along the water column (0–2000 m) in the central part of the NW Mediterranean Sea (Dyfamed site), *Deep Sea Res., Part II*, *49*(11), 2049–2066.

Dickson, A. G. (1990), Standard potential of the reaction - AgCl(s) + 1/2 H2(g) = Ag(s) + HCl(aq) and the standard acidity constant of the ion HSO_4^- in synthetic sea-water from 273.15 K to 318.15 K, *J. Chem. Thermodyn.*, *22*(2), 113–127.

Dickson, A. G. (1998), Reference material for oceanic carbon dioxide measurements, *CDIAC Commun.*, *25*, 1, 16.

Dickson, A. G., and F. J. Millero (1987), Comparison of the equilibrium-constants for dissociation of carbonic-acid in seawater, *Deep Sea Res., Part I*, *34*(10), 1733–1743.

Dickson, A. G., J. D. Afghan, and G. C. Anderson (2003), Reference materials for oceanic CO_2 analysis: A method for the certification of total alkalinity, *Mar. Chem.*, *80*(2–3), 185–197.

Friis, K., A. Körtzinger, and D. W. R. Wallace (2003), The salinity normalization of marine inorganic carbon chemistry data, *Geophys. Res. Lett.*, *30*(2), 1085, doi:10.1029/2002GL015898.

Gascard, J. C. (1978), Mediterranean deep-water formation baroclinic instability and oceanic eddies, *Oceanol. Acta*, *1*(3), 315–330.

Hiscock, W. T., and F. J. Millero (2006), Alkalinity of the anoxic waters in the western Black Sea, *Deep Sea Res., Part II*, *53*(17–19), 1787–1801.

Johnson, K. M., K. D. Wills, D. B. Butler, W. K. Johnson, and C. S. Wong (1993), Coulometric total CO_2 analysis for marine studies, *Mar. Chem.*, *44*(2–4), 167–187.

Klein, B., et al. (1999), The large deep water transient in the eastern Mediterranean, *Deep Sea Res., Part I*, *46*(3), 371–414.

Lascaratos, A., W. Roether, K. Nittis, and B. Klein (1999), Recent changes in deep water formation and spreading in the eastern Mediterranean Sea: A review, *Prog. Oceanogr.*, *44*(1–3), 5–36.

Lee, K., L. T. Tong, F. J. Millero, C. L. Sabine, A. G. Dickson, C. Goyet, G.-H. Park, R. Wanninkhof, R. A. Feely, and R. M. Key (2006), Global relationships of total alkalinity with salinity and temperature in surface waters of the world's oceans, *Geophys. Res. Lett.*, *33*, L19605, doi:10.1029/2006GL027207.

Lewis, E., and D. W. R. Wallace (1998), Program developed for CO_2 System Calculations, *ORNL/CDIAC-105*, http://cdiac.ornl.gov/oceans/co2rprt.html, Carbon Dioxide Inf. Anal. Cent., Oak Ridge Natl. Lab., U.S. Dep. of Energy, Oak Ridge, Tenn.

Martin, J., A. Palanques, and P. Puig (2006), Composition and variability of downward particulate matter fluxes in the Palamos submarine canyon (NW Mediterranean), *J. Mar. Syst.*, *60*(1–2), 75–97.

Mehrbach, C., C. Culberso, J. E. Hawley, and R. Pytkowic (1973), Measurement of apparent dissociation-constants of carbonic-acid in seawater at atmospheric-pressure, *Limnol. Oceanogr.*, *18*(6), 897–907.

Menard, H. W., and S. M. Smith (1966), Hypsometry of ocean basin provinces, *J. Geophys. Res.*, *71*(18), 4305–4325.

Millero, F. J., J. Morse, and C. T. Chen (1979), Carbonate system in the western Mediterranean Sea, *Deep Sea Res., Part I*, *26*(12), 1395–1404.

Mintrop, L., F. F. Perez, M. Gonzalez-Davila, M. J. Santana-Casiano, and A. Körtzinger (2000), Alkalinity determination by potentiometry: Intercalibration using three different methods, *Cienc. Mar.*, *26*(1), 23–37.

Ovchinnikov, I. M. (1984), Intermediate water formation in the Mediterranean Sea, *Oceanology*, *24*(2), 217–225.

Pollak, M. J. (1951), The sources of the deep water of the eastern Mediterranean Sea, *J. Mar. Res.*, *10*(1), 128–151.

Roether, W., et al. (1996), Recent changes in eastern Mediterranean deep waters, *Science*, *271*(5247), 333–335.

Tixeront, J. (1969), Le bilan hydrologique de la mer Noire et de la mer Méditerranée, *Bull. Int. Assoc. Sci. Hydrol.*, *14*(4), 61–69.

A. Körtzinger, A. Schneider, and D. W. R. Wallace, Forschungsbereich Marine Biogeochemie, Leibniz-Institut für Meereswissenschaften, IFM-GEOMAR, Düsternbrooker Weg 20, D-24105 Kiel, Germany. (aschneider@ifm-geomar.de)